Annals of Warsaw University of Life Sciences – SGGW
Forestry and Wood Technology № 114, 2021: 33-42
(Ann. WULS-SGGW, Forestry and Wood Technology 114, 2021: 33-42)

Raman Spectroscopy in the investigations of indexable knives for wood-based materials machining

MAREK BARLAK[1], JACEK WILKOWSKI[2], MAGDALENA WILCZOPOLSKA[1], ZBIGNIEW WERNER[1], BOGDAN STASZKIEWICZ[1], JERZY ZAGÓRSKI[1] (0000-0001-6311-947X)

[1]Plasma/Ion Beam Technology Division, Material Physics Department, National Centre for Nuclear Research Świerk, 7 Andrzeja Sołtana St., 05-400 Otwock, Poland;
[2]Department of Mechanical Processing of Wood, Institute of Wood Sciences and Furniture, Warsaw University of Life Sciences, 159 Nowoursynowska St., 02-776 Warsaw, Poland;

Abstract: *Raman spectroscopy for examination of WC-Co tools in wood-base machining.* An attempt is undertaken to apply Raman Spectroscopy for examination of WC-Co tools for wood-base machining. The virgin tools were compared with those implanted with nitrogen, modified by electron beam and plasma beam pulses. The preliminary results suggest a possibility of applying this method for fast, non-destructive analysis of phase composition and phase changes in the microstructure of the investigated tools

Keywords: Raman Spectroscopy, WC-Co indexable knives, tools modification

INTRODUCTION

Ceramic materials, such as: oxides, nitrides, borides, silicides, fluorides, carbides and carbon itself (Barlak et al. 2005, Olesińska et al. 2006, Chmielewski et al. 2017, Chmielewski et al. 2018), are often called leading materials or materials of the future. They find wide application in modern machinery and devices requiring featuring high performance and reliability. The ceramic tools replace the classic steel tools due to their greater durability. Unfortunately, their durability is still insufficient,and for this reason there are many investigations to improve this state (Kołodziejczak et al. 2017, Wilkowski et al. 2018, Barlak et al. 2019, Wilkowski et al. 2020, Barlak et al. 2020a, Barlak et al. 2020b, Morozow et al. 2021, Wilkowski et al. 2021). Apart from the development of modifications, the methods of the quick evaluation of the obtained results are sought. Raman Spectroscopy (Wilczopolska et al. 2021) seems to be a potential method, which can be used for this purpose. Raman Spectroscopy is widely used for the qualitative and quantitative analysis of solids, liquids and gases. It is a fast, non-destructive research method, exhibiting results accuracy and a large number of received information obtained at relatively low costs. Unfortunately, usually, this method is used in the investigation together with other methods for the phase composition evaluation i.e. X-Ray Diffraction Analysis (XRD) and/or X-ray Photoelectron Spectroscopy (XPS) or in the simplest case - together with Energy Dispersive X-ray Spectroscopy (EDS) - a method revealing elemental composition of the investigated material.

This paper shortly describes this method and presents examples of own research results, which were obtained on the virgin and the modified WC-Co indexable knives for wood-based materials machining.

METHODS AND MATERIALS

The commercially available, WC-Co indexable knives, produced by Ceratizit company (KCR08), with dimensions 29.5×12×1.5 mm3 and presented in Fig. 1, were used in the investigations.

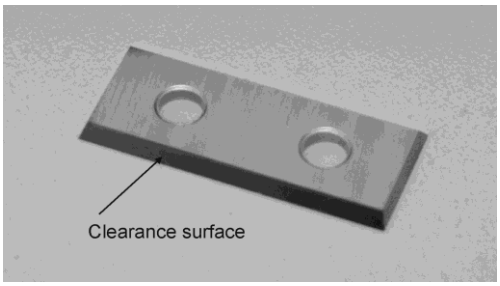

Figure 1. WC-Co indexable knive for wood-based material machining

The clearance surfaces of the investigated tools were treated using three methods:

1. ion implantation of nitrogen,
2. pulse electron treatment,
3. high-intensity plasma pulse treatment.

The ion implantation processes were described in Refs (Wilkowski et al. 2019, Barlak et al. 2019). The samples (knives) were implanted with nitrogen ions using a non-mass separated beam, generated by a semi-industrial implanter. Nitrogen of 99.999% purity was used as the source of the implanted ions. The implanted nitrogen was delivered as two kinds of ions, i.e. N^++N_2^+ in the ratio ~1:1. The implanted dose was 2e17 cm^{-2}. Ions were implanted at 60 kV acceleration voltage. The implanted samples (knives) were clamped onto a stainless steel plate to avoid overheating effects and the ion current densities were kept below 50 μA/cm^2, so the estimated value of temperature of the implanted samples did not exceeded 200°C. The working pressure in the vacuum chamber was at a level from 2 to 5e-3 Pa.

The use of pulse electron treatment method was presented e.g. in Refs (Werner et al. 2016, Werner et al. 2020). The samples were treated with electron-beam pulses generated by electron pulse gun. A single electron pulse was applied. The electron-beam pulse length was around 2 μs and the energy density was at a level of 6 J/cm^2. This value was homogeneous within 20% over a 50 mm diameter circle. The electron energy density was determined by a copper calorimeter with a thermistor temperature measurement, attached to the sample holder close to the sample. The acceleration voltage was 30 kV. Argon of 99.999% purity was used as a working gas. The working pressure in the vacuum chamber was at a level of 8e-2 Pa.

In the third case, the knives were treated using high-intensity plasma pulses generated by Rod Plasma Injector (RPI) type generator - IBIS. This method of the high-intensity plasma pulses was described in details in Ref. (Barlak 2010). 20 plasma pulses were applied. The pulse duration was about 1 μs. The energy density of each pulse was at a level of 6 J/cm^2. The base pressure in the vacuum chamber was at a level of 2.7e-3 Pa. Plasma injector worked in PID (Pulse Implantation Doping) mode.

The selected, modified samples showed the greatest durability for the given modification type.

In the next step, virgin (non-modified, non-treated) and the treated knives were analysed using Raman Spectroscopy. Few words about this method is presented below, because, this method is relatively new, especially in wood industry.

Figure 2 shows the idea of Raman Spectroscopy method.

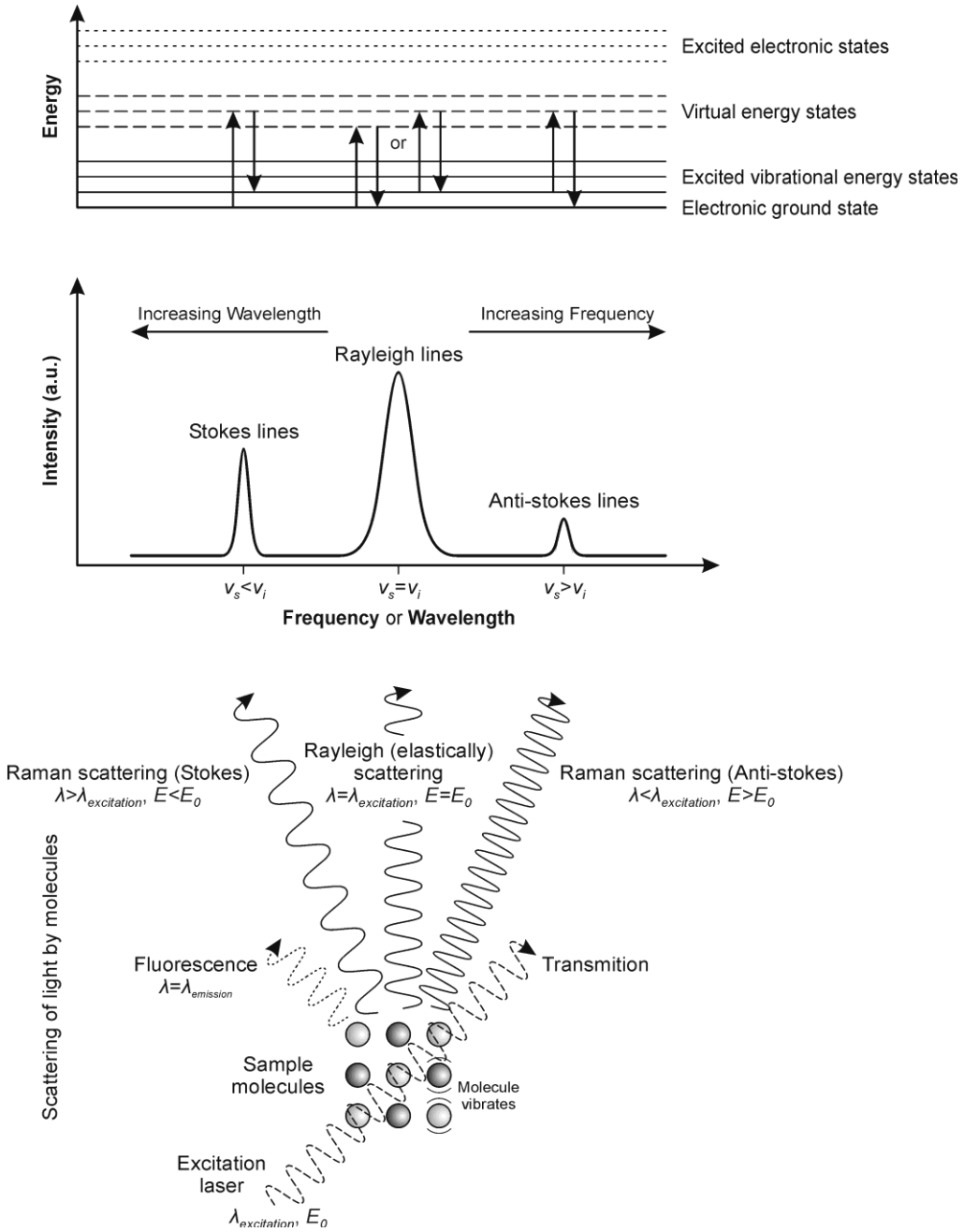

Figure 2. The idea of Raman Spectroscopy

The Raman Spectroscopy is based upon the effect of scattering caused by the interaction of electromagnetic radiation (originating from is a laser) with an oscillating molecule. Monochromatic and coherent radiation impinging the molecule, excites the molecule of the analyzed substance to a virtual energy level, from which they return to the ground vibrational state emitting photons of scattered radiation in all directions. Most of the scattered radiation is due to elastic scattering and is referred to as Rayleigh scattering. The small part of the scattered radiation that is related to a change in the energy of the photon (inelastic scattering) is referred to as Raman scattering. Scattering results in a dispersion of emission bands. The Rayleigh band is obtained when the scattered photons do not change frequency in relation to the incident photons. They do not match the energy levels of the molecule and cannot be absorbed, they are dispersed, and the molecule remains at the same energy level. The Stokes band is formed when the molecule after interaction with the radiation excitation, moves from the first excitation level to a lower oscillatory level and the scattered photon has the energy lower by the energy

difference of the vibrational energy levels hν. The Rayleigh band is separated from the Raman band by the oscillation frequency hν. The anti-Stokes band occurs if the molecule was at the excited oscillatory level before the action of the excitation radiation, then it goes to the excited virtual level and returns to the basic oscillatory level. The scattered photon will have energy greater by the energy difference of the vibrational energy levels *hν*. In the spectrum, we will then get a Raman band that is distant from the Rayleigh band by the oscillation frequency ν, but in the opposite direction than the Stokes band. In Raman spectroscopy, the measurement most often concerns the Stokes bands due to the fact that they are much stronger than the anti-Stokes bands, because at room temperature, most of the molecules, at which we record the spectra, are at the zero oscillation level.

The results of Raman spectroscopy studies were obtained using a confocal Raman microscope (WITec Alpha 300R, WITec, Germany) equipped with a laser Nd: YAG 532 nm and a spectrometer WITEC UHTS VIS-NIR with thermoelectrically cooled camera CCD. Raman Stokes signals were recorded with a lens with a magnification of 100× (Zeiss LD EC Epiplan-Neofluar Dic 100×/0.75) in the Raman shift range of 0 to 3500 cm^{-1}, with the laser power of 5 mW.

Detailed knowledge of the properties of different components of the sample was possible by Raman mapping technique. A multi-channel detector allowed to obtain information about both the spectra and the location of the measurement points. A Raman spectrum over the entire wavelength is recorded at each measured point. Further analysis consists in selecting an appropriate marker band and measuring its integral intensity, which leads to the construction of a Raman map showing the distribution of a specific compound in the tested sample. Mapping of knives has been done on the surface 100×100 μm^2, collecting information about spectra in 40 lines, with 40 points in each analyzed line. Map enabled to distinguish individual components of the sample.

RESULTS AND DISCUSSION

Figure 3 presents Raman spectra for the virgin WC-Co material, nitrogen ion implanted, electron pulse treated and plasma treated samples. The numbers from 1 to 14 indicate the identified peaks. The detail description of these peaks is presented in Table 1. The peak number is in the first column, the approximate position of the each peak - in the second column, the probable phase and the literature reference to the nearest peaks - in the third and fourth columns, respectively. The values of "Raman shift" preceded by a tilde character (~) are not a values precisely defined by the authors, but values read from the graphs.

The probable phases, cited by more than one author are shown in bold. These values were considered as the most likely in our cases. These are: $CoWO_4$ for the peak position of 2, 5 and 6, Co_3O_4 for 3, 7 and 9, WO_3 for 4 and W=O for 10. The probable phase for the peak position of 8 is debatable, because two different phases, i.e. WO_3 and WC are cited equally. No phase could be identified for the peak position of 11. Similarly, no "nitrogen" peaks were observed in the spectra obtained for nitrogen implanted sample.

Peak 1 (WO_3) is clearly observed for virgin and electron treated samples. The height increase of peaks 2 ($CoWO_4$) and 3 (Co_3O_4) are especially visible for ion implantation and even more - for plasma treatment. Peak 4 (WO_3) is observed for all considered cases. Peak 5 ($CoWO_4$) occurs in addition to the virgin material also in electron and plasma treated materials. Peak 6 (also $CoWO_4$) is present for all treated samples, while peak 7 (Co_3O_4) is clear only for the virgin and the electron treated knives. Additionally, this peak is narrower for the case of electron modification compared to the virgin sample, which may indicate greater crystallinity (lower amorphisation) of this phase. Disorder and symmetry breaking in Raman spectroscopy is highly dependent on crystal symmetry. Peaks 8 (WO_3 or debatable WC) and 9 ($CoWO_4$) are low in all presented cases. Peak 10, attributed to the stretching vibration mode of the W=O bond

(Granados-Fitch et al. 2019) is relatively high only for the virgin material. Additionally, it is most likely left shifted in the case of the plasma modification. Shift of the peak position is related to the formation of stress in the sample. The increase in the shift of the peak towards higher values is attributed to atomic dislocations and/or structural disturbances that cause compressive stresses, while the decrease in the shift of the peak is attributed to tensile stresses. In this case plasma modification causes compressive stresses in sample.

In conclusion, it can be said that the peaks from 1 to 10 indicate the presence of the various oxide phases in the investigated materials, usually independently of their treatment. The signal of the pure WC phase is debatable.

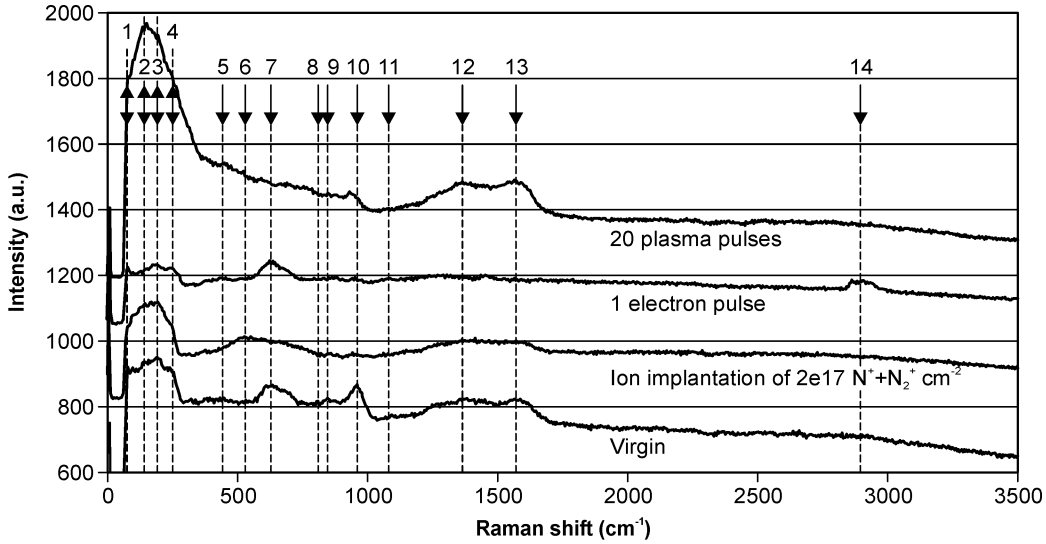

Figure 3. Raman spectra for virgin, ion implanted, electron and plasma pulse treated WC-Co materials

Table 1. The detail description of the peaks indicated from Raman spectra

Peak number	Raman shift (cm^{-1})	Probable phase	Reference
1	~70	WO_3	Myalska et al. 2019
2	~120	WC	Kamdi and Voisey 2015
	~140	W-O	Granados-Fitch et al. 2019
	~150	**$CoWO_4$**	Geng et al. 2015
	~150	**$CoWO_4$**	Myalska et al. 2019
3	190-330	W-O-W	Strunk et al. 2017
	~200	$CoWO_4$	Geng et al. 2015
	~200	**Co_3O_4**	
	~200	**Co_3O_4**	Myalska et al. 2019
4	~260	**WO_3**	Torgerson et al. 2018
	~270	$CoWO_4$	Geng et al. 2015
	~270	**WO_3**	
	~270	**WO_3**	Kamdi and Voisey 2015
	~270	**WO_3**	Katiyar and Randhawa 2019
	~270	**WO_3**	Myalska et al. 2019
	~270	W-O	Granados-Fitch et al. 2019
5	~410	**$CoWO_4$**	Geng et al. 2015
	~410	W-O	Granados-Fitch et al. 2019
	420	WO_3	Debus et al. 2016
	~420	**$CoWO_4$**	Myalska et al. 2019

Table 1. The detail description of the peaks indicated from Raman spectra - continued

Peak number	Raman shift (cm^{-1})	Probable phase	Reference
6	~530	Co_3O_4	Myalska et al. 2019
	~540	**$CoWO_4$**	
	~540	**$CoWO_4$**	Geng et al. 2015
	540	WO_3	Debus et al. 2016
7	~620	Co	Kamdi and Voisey 2015
	~620	**Co_3O_4**	Geng et al. 2015
	~620	**Co_3O_4**	Myalska et al. 2019
8	~800	**WC**	Kamdi and Voisey 2015
	~800	**WO_3/WC**	
	802-804	**WO_3**	Strunk et al. 2017
	805	**WC**	Mrabet et al. 2009
	~810	W-O	Granados-Fitch et al. 2019
	~810	**WO_3**	
9	~880	**$CoWO_4$**	Geng et al. 2015
	~880	**$CoWO_4$**	Myalska et al. 2019
	~880	WO_3	Katiyar and Randhawa 2019
	~880	W=O	Granados-Fitch et al.2019
	879.5	**WO_4^{2-}**	Liu et al. 2017
	881.2		
10	~940-985	$WO_4(aq)+W_{12}O_{39}(aq)$	Strunk et al. 2017
	961	**W=O**	
	967-973		
	960-990		
	948.2	**W=O**	Liu et al. 2017
	960	**W=O**	Mrabet et al. 2009
	~960	WO_32H_2O	Myalska et al. 2019
	~980		
	970	**W=O**	Debus et al. 2016
	~980	**W=O**	Granados-Fitch et al. 2019
11	~1080	?	-
12	1298	G band	Cheong et al. 2017
	1335		
	~1350	Amorphous C	Myalska et al. 2019
	1350	Disordered C	Liu et al. 2017
	1351		
	1351	D band	Veerakumar et al. 2017
	1353.2	D bands for graphitic carbon	Wei et al. 2010
	1354.1		
	1356.4		
	1359	Graphite	Abbas and Musa 2019
	1360	D band	Debus et al. 2016

Table 1. The detail description of the peaks indicated from Raman spectra - continued

13	1566.7	G band for sp^2sites	Wei et al. 2010
	1567.3		
	1552.7		
	1580	G band	Debus et al. 2016
	1580	Graphite	Abbas and Musa 2019
	~1580	Amorphous C	Myalska et al. 2019
	1582	D band	Cheong et al. 2017
	1597		
	1584	G line	Mrabet et al. 2009
	1594		
	1598	G band	Veerakumar et al. 2017
14	2902	D+G band	Veerakumar et al. 2017
	~2700	C-H	Kosińska et al. 2020

Peaks 12 (D), 13 (G) and 14 (D+G) are assigned to different forms of carbon. D- and G-modes related to the graphite is an indication of graphitization (Debus et al. 2016, Zkria et al. 2019). G label applies to graphite and D band is observed in the presence of defects, hence the name is D for defect or disorder. However, it is worth noting that there are no homogeneity of attributing these peaks in the literature (see Table 1).

Peaks 12 and 13 are enhanced for ion implantation case and distinctly - for plasma treatment case. These peaks were missing for the electron treated material, but in this case we can see new peak, marked as "14", which is absent in all other spectra. There is a discrepancy in the identification of these peak. P. Veerakumar in Ref. (Veerakumar et al. 2017) suggest D+G band, while A. Kosińska in Ref. (Kosińska et al. 2020) shows it as a stretching vibrations, typical for carbon materials.

In our previous paper (Wilkowski et al. 2021) we presented a key role of carbon, which is known as the lubricating element, in improving the durability of the modified knives. There is some regularity between the presence and the height of the peaks and the durability of the tools. Peaks 12 and 13 are the highest for plasma treatment case - the durability increase for this case was more than threefold (the average value of Relative index of tool life was 3.01). The same peaks for nitrogen ion implanted can be related to the knives durability improvement at the level of 100% (Barlak et al. 2019). In the case of the electron treated samples, Relative index of tool life was about 1.73. Probably, it has to do with appearance of carbon peak 14.

The mentioned above carbon peaks and their relative intensity, can be used in the next step, to a more precise knowledge of the microstructure of the investigated materials, which is reported in Refs (Shen et al. 2016, Härmas et al. 2021).

CONCLUSIONS

The obtained Raman Spectroscopy results indicate that this method can be used for a quick, tentative investigation of WC-Co tools for wood-based materials machining. This method is suitable for the preliminary estimation/evaluation of the occurring phase changes, especially the graphitization process, which influencing an increase of the lubrication effect - one of the several main mechanisms of increasing durability of the tools. For a more detailed analysis, it is necessary to use additional methods to assess the phase and/or elemental composition, which is common practice in the scientific research.

REFERENCES

1. ABBAS R.K., MUSA K.M., 2019: Using Raman shift and FT-IR spectra as quality indices of oil bit PDC cutters, Petroleum, 5; 329-334. DOI: 10.1016/j.petlm.2018.10.003
2. BARLAK M., 2010: High intensity plasma pulses in ceramic wettability improvement, Instytut Problemów Jądrowych im. Andrzeja Sołtana. ISBN: 978-83-931455-0-8
3. BARLAK M., OLESIŃSKA W., PIEKOSZEWSKI J., CHMIELEWSKI M., JAGIELSKI J., KALIŃSKI D., WERNER Z., SARTOWSKA B., 2005: Ion implantation as a pre-treatment method of AlN substrate for direct bonding with copper, Vacuum 78; 205-209. DOI: 10.1016/j.vacuum.2005.01.027
4. BARLAK M., WILKOWSKI J., SZYMANOWSKI K., CZARNIAK P., PODZIEWSKI P., WERNER Z., ZAGÓRSKI J., STASZKIEWICZ B., 2019: Influence of the ion implantation of nitrogen and selected metals on the lifetime of WC-Co indexable knives during MDF machining., Annals of Warsaw University of Life Sciences - SGGW, Forestry and Wood Technology, 108; 45-52.
5. BARLAK M., WILKOWSKI J., WERNER Z., STASZKIEWICZ B., ZAGÓRSKI J., ZIÓŁKOWSKI K., 2020a: Biuletyn Informacyjny OB-RPPD, 3-4; 167-177. 10.32086/biuletyn.2020.07, in Polish
6. BARLAK M., WILKOWSKI J., WERNER Z., ZAGÓRSKI J., STASZKIEWICZ B., SZKARŁAT F., 2020b: The influence of the CO_2 ion implantation on the life-time of WC-Co tools used in wood materials machining, Biuletyn Informacyjny OB-RPPD, 3-4; 178-187. 10.32086/biuletyn.2020.08, in Polish
7. CHEONG Y.-K., CALVO-CASTRO J., CIRIC L., EDIRISINGHE M., CLOUTMAN-GREEN E., ILLANGAKOON U.E., KANG Q., MAHALINGAM S., MATHARU R.K., WILSON R.M., REN G., 2017: Characterisation of the chemical composition and structural features of novel antimicrobial nanoparticles, Nanomaterials, 7; 152. DOI: 10.3390/nano7070152
8. CHMIELEWSKI M., NOSEWICZ S., KURPASKA Ł., ROMELCZYK B., 2016: Evolution of material properties during the sintering process of Cr-Re-Al_2O_3 composites, Composites Part B, 98; 88-96. DOI: 10.1016/j.compositesb.2016.04.065
9. CHMIELEWSKI M., PIETRZAK K., TEODORCZYK M., NOSEWICZ S., JARZĄBEK D., ZYBAŁA R., BAZARNIK P., LEWANDOWSKA M., STROJNY-NEDZA A., 2017: Effect of metallic coating on the properties of copper-silicon carbide composites, Applied Surface Science, 421A; 159-169. DOI: 10.1016/j.apsusc.2016.12.130
10. DEBUS J., SCHINDLER J.J., WALDKIRCH P., GOEKE S., BRÜMMER A., BIERMANN D., BAYER M., 2016: Indication of worn WC/C surface locations of a dry-running twin-screw rotor by the oxygen incorporation in tungsten-related Raman modes, Applied Physics Letters 109; 171601. DOI: 10.1063/1.4966145
11. GENG Z., LI S., DUAN D.L., LIU Y., 2015: Wear behaviour of WC-Co HVOF coatings at different temperatures in air and argon, Wear, 330-331; 348-353. DOI: 10.1016/j.wear.2015.01.035
12. GRANADOS-FITCH M.G., QUINTANA-MELGOZA J.M., JUAREZ-ARELLANO E.A., AVALOS-BORJA M., 2019: Degradation of rhenium carbide obtained by mechanochemical synthesis at oxygen and moisture environmental conditions, Materials Chemistry and Physics, 229; 15-21. DOI: 10.1016/j.matchemphys.2019.02.088

13. HÄRMAS R., PALM R., KURIG H., PUUSEPP L., PFAFF T., ROMANN T., ARUVÄLI J., TALLO I., THOMBERG T., JÄNES A., LUST E., 2021: Carbide-derived carbons: WAXS and Raman spectra for detailed structural analysis, Journal of Carbon Research, 7; DOI: 10.3390/c7010029
14. KAMDI Z., VOISEY K.T., 2015: Characterization of WC-Co coatings corrosion product by Raman Spectroscopy, Advanced Materials Research, 1087; 379-383. DOI: 10.4028/www.scientific.net/AMR.1087.379
15. KATIYAR P.K., RANDHAWA N.S., 2019: Corrosion behavior of WC-Co tool bits in simulated (concrete, soil, and mine) solutions with and without chloride additions, International Journal of Refractory Metals and Hard Materials, 85; 105062. DOI: 10.1016/j.ijrmhm.2019.105062
16. KOŁODZIEJCZAK P., WILKOWSKI J., BARLAK M., CZARNIAK P., WERNER Z., ZAGÓRSKI J., 2017: Modification of the surfaces of wood cutting tools using CO_2 laser - SEM analysis, Annals of Warsaw University of Life Sciences - SGGW, Forestry and Wood Technology, 98; 48-52.
17. KOSIŃSKA A., JAGIELSKI J., WILCZOPOLSKA M., BIELIŃSKI D., OKRASKA M., JÓŹWIK I., KURPASKA L., NOWAKOWSKA-LANGIER K., 2020: Study of the electrical properties of ion irradiated polymer materials, Surface and Coatings Technology, 388; 125562. DOI: 10.1016/j.surfcoat.2020.125562
18. LIU Y., CHENG J., YIN B., ZHU S., QIAO Z., YANG J., 2017: Study of the tribological behaviors and wear mechanisms of WC-Co and WC-Fe_3Al hard materials under dry sliding condition, Tribology International, 109; 19-25. DOI: 10.1016/j.triboint.2016.12.023
19. MOROZOW D., BARLAK M., WERNER Z., PISAREK M., KONARSKI P., ZAGÓRSKI J., RUCKI M., CHAŁKO L., ŁAGODZIŃSKI M., NAROJCZYK J., KRZYSIAK Z., CABAN J., 2021: Wear resistance improvement of cemented tungsten carbide deep-hole drills after ion implantation, Materials, 14; 239. 10.3390/ma14020239
20. MRABET S.E., ABAD M.D., LÓPEZ-CARTES C., MARTÍNEZ-MARTÍNEZ D., SÁNCHEZ-LÓPEZ J.C., 2009: Thermal evolution of WC/C nanostructured coatings by Raman and in situ XRD analysis, Plasma Processes and Polymers, 6; S444-S449. DOI: 10.1002/ppap.200931004
21. MYALSKA H., LUSVARGHI L., BOLELLI G., SASSATELLI P., MOSKAL G., 2019: Tribological behavior of WC-Co HVAF-sprayed composite coatings modified by nano-sized TiC addition, Surface and Coatings Technology, 371; 401-416. DOI: 10.1016/j.surfcoat.2018.09.017
22. OLESIŃSKA W., KALIŃSKI D., CHMIELEWSKI M., DIDUSZKO R., WŁOSIŃSKI W., 2006: Influence of titanium on the formation of a "barrier" layer during joining an AlN ceramic with copper by the CDB technique, Journal of Materials Science: Materials in Electronics 17; 781-788. DOI: 10.1007/s10854-006-0024-1
23. SHEN Y., LI L., XI J., QIU X., 2016: A facile approach to fabricate free-standing hydrogen evolution electrodes: riveting tungsten carbide nanocrystals to graphite felt fabrics by carbon nanosheets, Journal of Materials Chemistry A, 4; 5817-5822. DOI: 10.1039/c6ta01236a
24. TORGERSON T.B., HARRIS M.D., ALIDOKHT S.A., SCHARF T.W., AOUADI S.M., CHROMIK R.R., ZABINSKI J.S., VOEVODIN A.A., 2018; Room and elevated temperature sliding wear behavior of cold sprayed Ni-WC composite coatings, Surface and Coatings Technology, 350; 136-145. DOI: 10.1016/j.surfcoat.2018.05.090
25. VEERAKUMAR P., THANASEKARAN P., LIN K.-Ch., LIU S.-B., 2017: Well-dispersed rhenium nanoparticles on three-dimensional carbon nanostructures: Efficient

catalysts for the reduction of aromatic nitro compounds, Journal of Colloid and Interface Science, 506; 271-282. DOI: 10.1016/j.jcis.2017.07.065
26. WILCZOPOLSKA M., NOWAKOWSKA-LANGIER K., OKRASA S., SKOWRONSKI L., MINIKAYEV R., STRZELECKI G.W., CHODUN R., ZDUNEK K., 2021: Synthesis of copper nitride layers by the Pulsed Magnetron Sputtering method carried out under various operating conditions, Materials, 14; 2694. DOI: 10.3390/ma14102694
27. WILKOWSKI J., BARLAK M., WACHOWICZ J., BÖTTGER R., WERNER Z., 2018: The wear curves of nitrogen-implanted WC-Co indexable knives during particleboard milling, Annals of Warsaw University of Life Sciences - SGGW, Forestry and Wood Technology, 104; 395-399.
28. WILKOWSKI J., BARLAK M., WERNER Z., ZAGÓRSKI J., CZARNIAK P., PODZIEWSKI P., SZYMANOWSKI K., 2019: Technical note: Lifetime improvement and the cutting forces in nitrogen-implanted drills during wood-based material machining, Wood and Fiber Science, 51; 1-12. DOI: 10.22382/wfs-2019-021
29. WILKOWSKI J., BARLAK M., JAŁOCHA R., WERNER Z., AURIGA A., 2020: Analysis of sliding friction of WC-Co composite on particleboard, Annals of Warsaw University of Life Sciences - SGGW, Forestry and Wood Technology, 111; 60-67.
30. WILKOWSKI J., BARLAK M., BÖTTGER R., WERNER Z., KONARSKI P., PISAREK M., WACHOWICZ J., VON BORANY J., AURIGA A., 2021: Effect of nitrogen ion implantation on the life time of WC-Co tools used in particleboard milling, Wood Material Science and Engineering, 10.1080/17480272.2021.1900391
31. WERNER Z., BARLAK M., RATAJCZAK R., KONARSKI P., MARKOV A., HELLER R., 2016: Electron-beam pulse annealed Ti-implanted GaP, Journal of Applied Physics, 120; 085103. DOI: 10.1063/1.4961518
32. WERNER Z., BARLAK M., DŁUŻEWSKI P., HELLER R., PISAREK M., MARKOV A., PROSKUROWSKY D., 2020: Crystallographic changes in electron pulse annealing of Ti-implanted GaP, Radiation Effects and Defects in Solids, 175; 719-729. DOI: 10.1080/10420150.2020.1756814
33. ZKRIA A., HAQUE A., EGIZA M., ABUBAKR E., MURASAWA K., YOSHITAKE T., NARAYAN J., 2019: Laser-induced structure transition of diamond-like carbon coated on cemented carbide and formation of reduced graphene oxide, MRS Communications, 1-6. DOI: 10.1557/mrc.2019.88

Streszczenie: *Spektroskopia Ramana w badaniach narzędzi WC-Co wykorzystywanych w obróbce materiałów drzewnych.* W pracy podjęto próbę zastosowania Spektroskopii Ramana w badaniach wymiennych noży WC-Co, stosowanych do obróbki materiałów drewnopochodnych. Przeanalizowano narzędzia niezmodyfikowane, implantowane jonami azotu, poddane działaniu impulsów elektronowych i plazmowych. Wstępne wyniki sugerują możliwość zastosowania tej metody do szybkiej i nieniszczącej analizy składu fazowego i zmian fazowych w mikrostrukturze badanych narzędzi.

Corresponding author:

Marek Barlak
7 Andrzeja Sołtana St.
05-400 Otwock, Poland
email: marek.barlak@ncbj.gov.pl
phone: +48 22 273 16 44